Radio emission and jets from microquasars

Elena Gallo

Hubble Fellow at the MIT Kavli Institute for Astrophysics and Space Research,
70 Vassar Street, Bldg 37-685, Cambridge, MA 02139, USA

Summary. To some extent, all Galactic binary systems hosting a compact object are potential 'microquasars', so much as all galactic nuclei may have been quasars, once upon a time. The necessary ingredients for a compact object of stellar mass to qualify as a microquasar seem to be: accretion, rotation and magnetic field. The presence of a black hole may help, but is not strictly required, since neutron star X-ray binaries and dwarf novae can be powerful jet sources as well. The above issues are broadly discussed throughout this Chapter, with a a rather trivial question in mind: why do we care? In other words: are jets a negligible phenomenon in terms of accretion power, or do they contribute significantly to dissipating gravitational potential energy? How do they influence their surroundings? The latter point is especially relevant in a broader context, as there is mounting evidence that outflows powered by super-massive black holes in external galaxies may play a crucial role in regulating the evolution of cosmic structures. Microquasars can also be thought of as a form of quasars for the impatient: what makes them appealing, despite their low number statistics with respect to quasars, are the fast variability time-scales. In the first approximation, the physics of the jet-accretion coupling in the innermost regions should be set by the mass/size of the accretor: stellar mass objects vary on $10^5 - 10^8$ times shorter time-scales, making it possible to study variable accretion modes and related ejection phenomena over average Ph.D. time-scales. At the same time, allowing for a systematic comparison between different classes of compact objects – black holes, neutron stars and white dwarfs – microquasars hold the key to identify and characterize properties that may be unique to, e.g., the presence (or lack) of an event horizon.

1 Radio observations of black holes

The synchrotron nature of the radio emission from X-ray binaries is generally inferred by the non-thermal spectra and high brightness temperatures. The latter translate into minimum linear sizes for the radio emitting region which often exceed the typical orbital separations, making the plasma uncontainable by any known component of the binary. If coupled to persistent radio flux levels, this implies the presence of a continuously replenished relativistic plasma that is flowing out of the

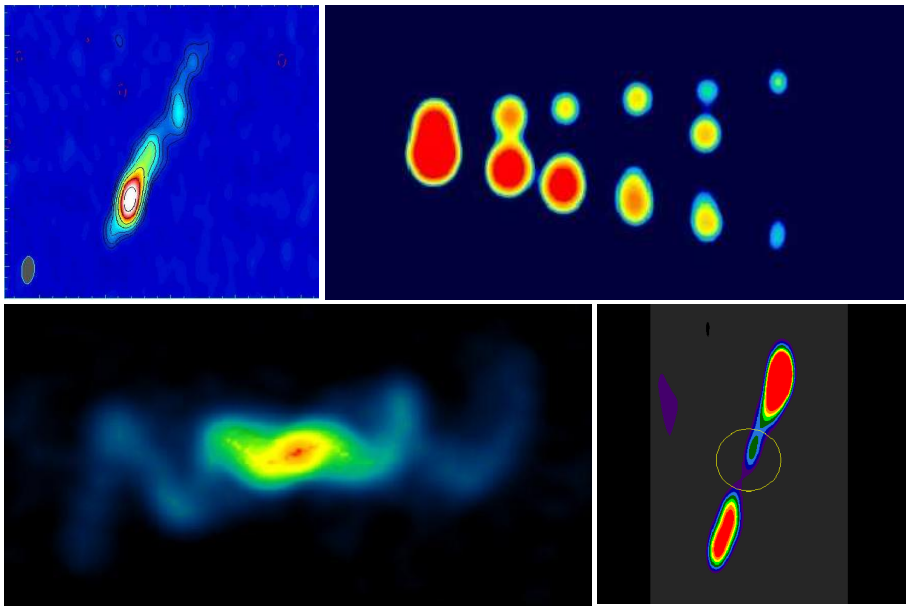

Fig. 1. Top left: steady, milliarcsec scale jet from the high mass black hole X-ray binary Cyg X-1. From [114]. Top right: transient, arcsec-scale radio jets from the superluminal Galactic jet source GRS 1915+105. From [98]. Bottom left: arcsec-scale radio jets from the first Galactic source discovered: SS 443. The binary orbit is almost edge-on; the precessing accretion disk of SS 433 causes its jets to trace a 'corkscrew' in the sky every 162 days. From [12]. Bottom right: fossil, arcmin-scale radio jets around the Galactic Center black hole in 1E 140.7-2942. From [99].

system [58, 95, 30]. Thanks to aggressive campaigns of multi-wavelength observations of X-ray binaries in outbursts over the last decade or so, we have now reached a reasonable understanding of their radio phenomenology in response to global changes in the accretion mode.

For the black holes (BHBs), radiatively inefficient, low/hard X-ray states are associated with flat/slightly inverted radio-to-mm spectra and persistent radio flux [39] (the reader is referred to Chap. 3 of this book for a review of X-ray states of black hole X-ray binaries, as well as: [80, 60]). In analogy with compact extragalactic radio sources, the flat spectra are thought to be due to the superimposition of a number of peaked synchrotron spectra generated along a conical outflow, or jet, with the emitting plasma becoming progressively thinner at lower frequencies as it travels away from the jet base [11, 69]. The jet interpretation has been confirmed by high resolution radio maps of two hard state BHBs: Cygnus X-1 [114] (Fig. 1, top left panel) and GRS 1915+105 [25, 42] are both resolved into elongated radio sources on milliarcsec-scales (tens of A.U.) implying collimation angles smaller than a few degrees. Even though no collimated radio jet has been resolved in any BHB emitting X-rays below a few % of the Eddington limit, $L_{\rm Edd}$, it is widely accepted, by analogy with the two above-mentioned systems, that the flat radio spectra associated with unresolved radio counterparts of X-ray binaries are originated in conical outflows.

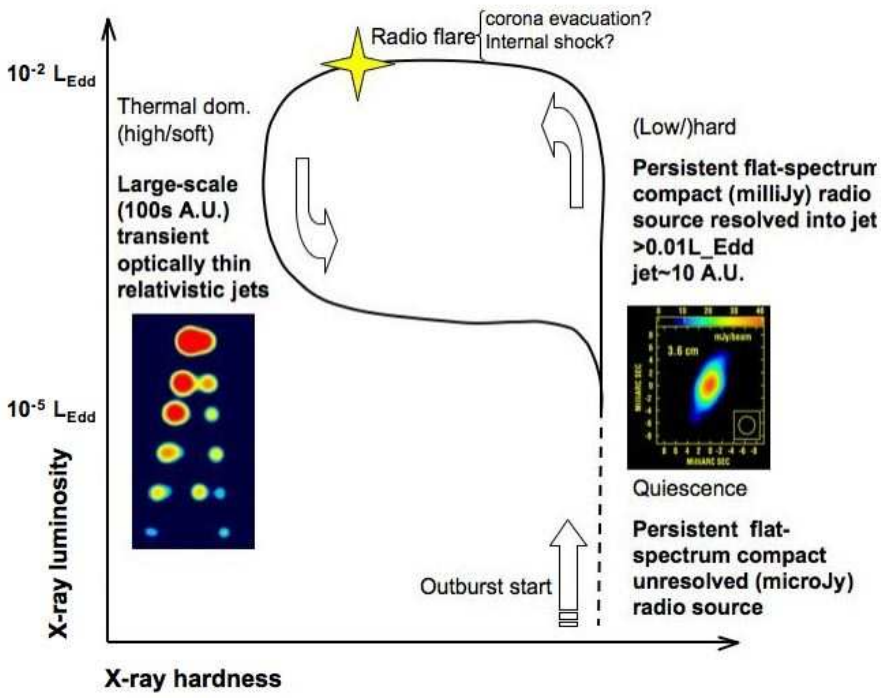

Fig. 2. Schematic of radio properties of black hole X-ray binaries over different accretion modes (see Chap. 3 for a description of X-ray states). See: `http://www.issibern.ch/teams/proaccretion/Documents.html` for a more detailed illustration, and [34, 32] for the relative science papers.

Yet, it remains to be proven whether such outflow would maintain highly collimated at very low luminosity levels, in the so called 'quiescent' regime ($L_X/L_{Edd} \lesssim 10^{-5}$; see Sect. 5.1).

Radiatively efficient, high/soft (thermal dominant) X-ray states, on the contrary, are associated with no *flat spectrum* core radio emission [41]; the core radio fluxes drop by a factor at least 50 with respect to the hard state (e.g. [41, 18]), which is generally interpreted as the physical suppression of the jet taking place over this regime. While a number of sources has been detected in the radio during the soft state [14, 18, 48, 13], the common believe is that these are due to optically thin synchrotron emission – until proven otherwise.

Transient ejections of optically thin radio plasmons moving away from the binary core in opposite directions are often observed as a result of bright radio flares associated with hard-to-soft X-ray state transitions (Fig. 1, top right panel). This are surely the most spectacular kind of jets observed from X-ray binaries, in fact those which have inspired the term 'microquasar' [96]. As proven by the case of GRS 1915+105, and more recently by Cygnus X-1 as well [31], the same

source can produce either kind of jets, persistent/partially self-absorbed, and transient/optically thin, dependently on the accretion regime.

2 Coupling accretion and ejection in black holes

The question arises weather the flat-spectrum, steady jet and the optically-thin discrete ejections differ fundamentally or they are different manifestations of the same phenomenon. This issue has been tentatively addressed with a phenomenological approach [34]. Broadly speaking, this model aims to put together the various pieces of a big puzzle that were provided to us by years of multi-wavelength monitoring of BHBs, and to do so under the guiding notion that the jet phenomenon has to be looked at as an intrinsic part of the accretion process. [34] collected as many information as possible about the very moment when major radio flares occur in BHBs, and proposed a way to 'read them' in connection with the X-ray state over which they took place as well as the observed jet properties prior and after the radio flare.

The study makes use of simultaneous X-ray (typically Rossi X-ray Timing Explorer, RXTE) and radio (Australia Telescope Compact Array, ATCA, and/or the Very Large Array, VLA) observations of four outbursting BHB systems: GRS 1915+105, XTE J1550-564, GX 339-4 and XTE J1859+229. X-ray hardness-intensity diagrams (HID) have been constructed for the various outbursts and linked with the evolution of the jet morphology, radio luminosity, total power, Lorentz factor and so on.

Figure 2 (naively) illustrates our understanding of the so called jet-accretion coupling in BH X-ray binaries. It represents the HID of a well behaved outburst, with the time arrow progressing counterclockwise. Starting from the bottom right corner, the system is a low-luminosity, quiescent X-ray state, producing a (supposedly) mildly relativistic, persistent outflow, with flat radio spectrum. Its luminosity starts to increase at all wavelengths, while the X-ray spectrum remains hard. Around a few % of the Eddington X-ray luminosity, a sudden transition is made (top horizontal branch) during which the global properties of the accretion flow change substantially (hard-to-soft state transition), while a bright radio flare is observed, likely due to a sudden ejection episode [97]. This can be interpreted [34] as the result of the inner radius of a geometrically thin accretion disk moving inward. The Lorentz factor of the ejected material, due to the deeper potential well, exceeds that of the hard state jet, causing an internal shock to propagate through it, and to possibly disrupt it. Once the transition to the high/soft (thermal dominant) state is made, no core radio emission is observed, while large scale (hundreds of A.U.), rapidly fading radio plasmons are often seen moving in opposite direction with respect to the binary system position, with highly relativistic speed. Towards the end of the outburst, the X-ray spectrum starts to become harder, and the compact, flat-spectrum, core radio source turns on once again. A new cycle begins (with time-scales that vary greatly from source to source).

The bright radio flare associated with the state transition could coincide with the very moment in which the hot corona of thermal electrons, responsible for the X-ray power law in the spectra of hard state BHBs, is accelerated and ultimately evacuated. This idea of a sudden evacuation of inner disk material is not entirely new, and in fact dates back to extensive RXTE observations of the rapidly varying

GRS 1915+105: despite their complexity, the source spectral changes could be accounted for by the rapid removal of the inner region of an optically thick accretion disk, followed by a slower replenishment, with the time-scale for each event set by the extent of the missing part of the disk [7, 8]. Subsequent, multi-wavelength (radio, infrared and X-ray) monitoring of the same source suggested a connection between the rapid disappearance and follow up replenishment of the inner disk seen in the X-rays, with the infrared flare starting during the recovery from the X-ray dip, when an X-ray spike was observed [97].

Yet it remains unclear what drives the transition in the radio properties after the hard X-ray state peak is reached. Specifically, radio observations of GX 339-4, XTE J1550-564 and GRS 1915+105 indicate that in this phase the jet spectral index seems to 'oscillate' in an odd fashion, from flat to inverted to optically thin, as if the jet was experiencing some kind of instability as the X-ray spectrum softens. Recent, simultaneous RXTE and INTEGRAL (The INTernational Gamma-Ray Astrophysics Laboratory) observations of GX 339-4 [6] have shown that the high energy cutoff typical of hard state X-ray spectra, either disappears or shifts towards much higher energies within timescales of hours (<8 hr) during the transition.

Finally, there are at least a couple of recent results that might challenge some of the premises the unified scheme is based on. The first one is the notion that, for the internal shock scenario to be at work and give rise to the bright radio flare at the state transition, whatever is ejected must have a higher velocity with respect to the pre-existing hard state steady jet. From an observational point of view, this was supported, one one side, by the lower limits on the transient jets' Lorentz factors, typically higher than Γ=2 [35], and, on the other hand, by the relative small scatter about the radio/X-ray correlation in hard state BHBs [49] (see Sect. 3.1). The latter has been challenged on theoretical grounds [56].

The second premise has to do with the existence of a geometrically thin accretion disk in the low/hard state of BHBs. Deep X-ray observations of hard state BHBs [84, 85, 110, 116] (see also [52]). have shown evidence for a cool disk component extending close to the innermost stable orbit already during the bright phases of the hard state, that is prior to the horizontal brunch in the top panel of Fig. 2 ($L_X/L_{Edd} \simeq 10^{-3} - 10^{-2}$). This challenges the hypothesis of a sudden deepening of the inner disk potential well as the cause of a high Lorentz factor ejection. Possibly, whether the inner disk radius moves close to hole prior or during the softening of the X-ray spectrum does not play such a crucial role in terms of jet properties; if so, then the attention should be diverted to a different component, such as the presence/absence, or the size, of a Comptonizing corona [62], which could in fact coincide with the very jet base [76]. It is worth mentioning that a recent paper [67] gives theoretical support to the survival of a thin accretion disk down to low Eddington ratios: within the framework of the disk evaporation model (e.g. [66]), it is found that a weak, condensation-fed, inner disk can be present in the hard state of black hole transient systems for Eddington-scaled luminosities as low as 10^{-3} (depending on the magnitude of the viscosity parameter).

Here I wish to stress that, in addition to solving the above-mentioned issues, much work needs to be done in order to test the consistency of the internal shock scenario as a viable mechanism to account for the observed changes in the radio

properties, given the observational and theoretical constraints for a given source (such as emissivities, radio/infrared delays, cooling times, etc.).

Finally, one of the most interesting aspects of the proposed scheme – assuming that is correct in its general principles – is obviously its connection to super-massive BHs in active galactic nuclei (AGN), and the possibility to mirror different X-ray binary states into different classes of AGN. This is explored in detail in Chap. 5.

3 Empirical luminosity correlations

3.1 Radio/X-ray

In a first attempt to quantify the relative importance of jet vs. disk emission in BHBs, [49] collected quasi-simultaneous radio and X-ray observations of ten low/hard state sources. This study established the presence of a tight correlation between the X-ray and the radio luminosity, of the form $L_R \propto {L_X}^{0.7\pm0.1}$, first quantified for GX 339-4 [19]. The correlation extends over more than 3 orders of magnitude in L_X and breaks down around $2\%L_{Edd}$, above which the sources enter the high/soft (thermal dominant) state, and the core radio emission drops below detectable levels. Given the non-linearity, the ratio radio-to-X-ray luminosity increases towards quiescence (below a few $10^{-5}L_{Edd}$). This leads to the hypothesis that the total power output of quiescent BHBs could be dominated by a radiatively inefficient outflow, rather than by the local dissipation of gravitational energy in the accretion flow [37, 74].

Even though strictly simultaneous radio/X-ray observation of the nearest quiescent BHB, A 0620-00, seems to confirm that the non-linear correlation holds down to Eddington ratios as low as 10^{-8} [46], many outliers have been recently been found at higher luminosities [18, 16, 13, 15, 106, 45], casting serious doubts on the universality of this scaling, and the possibility of relying on the best-fitting relation for estimating other quantities, such as distance or black hole mass.

3.2 Optical-Infrared/X-ray

The infrared (IR) spectra of BHBs with a low mass donor star are likely shaped by a number of competing emission mechanisms, most notably: reprocessing of accretion-powered X-ray and ultraviolet photons, either by the donor star surface or by the outer accretion disk, direct thermal emission from the outer disk, and non-thermal synchrotron emission from a relativistic outflow. [109] have collected all the available quasi-simultaneous optical and near-IR data of a large sample of Galactic X-ray binaries over different X-ray states. The optical/near-IR (OIR) luminosity of hard/quiescent BHBs is found to correlate with the X-ray luminosity to the power $\sim$0.6, consistent with the radio/X-ray correlation slope down to $10^{-8}L_{Edd}$ [46]. Combined with the fact that the near-IR emission is largely suppressed in the soft state, this leads to the conclusion that, for the BHBs, the spectral break to the optically thin portion of the jet takes place most likely in the mid-IR (2-40 μm). A similar correlation is found in neutron stars (NSs) in the hard state. By comparing the observed relations with those expected from models of a number of emission processes, [109] are able to constrain the dominant contribution to the OIR portion

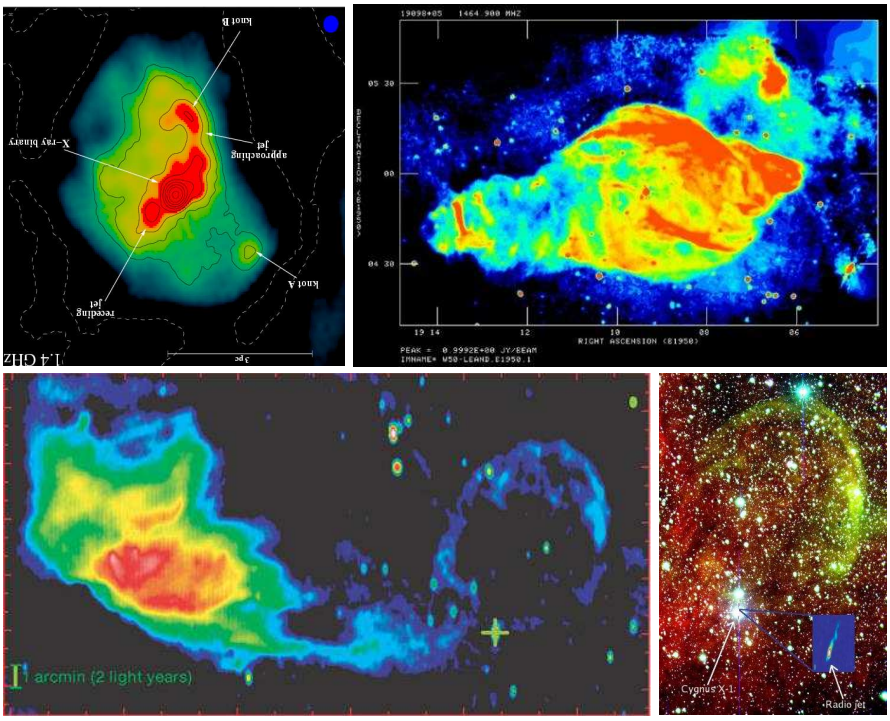

Fig. 3. Top left: the jet-powered radio nebula of the 'microblazar' Circinus X-1, imaged with the Australia Telescope Compact Array; from [119]. Top right: W50 nebula surrounding SS 433 (see Fig. 1, bottom left panel, for an image of the arcsec-scale radio jets). The jets of SS 433 are drilling their way into the supernova remnant, and give rise to these characteristic 'ears' [27]. Bottom left: a jet-powered radio nebula around the black hole X-ray binary Cygnus X-1, as seen by the Westerbork Synthesis Radio Telescope at 1.4 GHz. From [47]. Bottom right: the optical counterpart to the Cyg X-1 nebula, as observed with the 2.5m Isaac Newton optical telescope. From [108].

of the spectral energy distribution (SED) for the different classes of X-ray binaries. They conclude that, for hard state BHs at high luminosities (above 10^{-3} times the Eddington limit), jets are contributing 90% of the near-IR emission. The optical emission could have a substantial jet contribution; however, the optical spectra show a thermal spectrum indicating X-ray reprocessing in the disk dominates in this regime. In contrast, X-ray reprocessing from the outer accretion disk dominates the OIR spectra of hard state NSs, with possible contributions from the synchrotron emitting jets and the viscously heated disk only at very high luminosities.

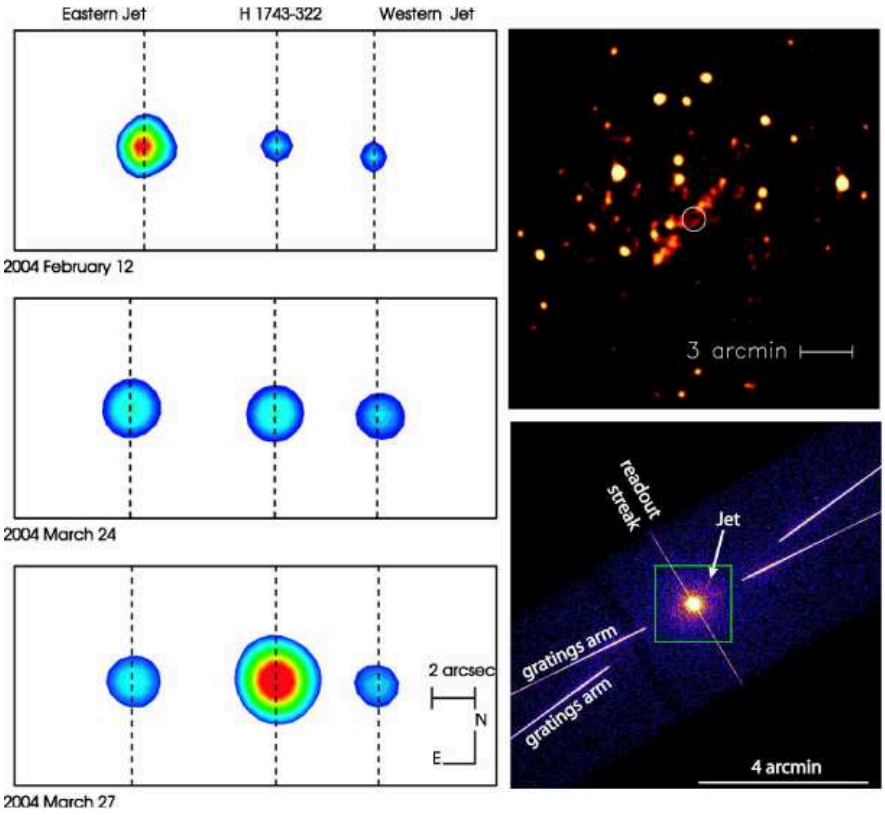

Fig. 4. Left panels: arcsec-scale, transient X-ray plasmons ejected by the BH candidate H 1743-322 (Chandra ACIS-S). The detection of optically thin synchrotron X-ray emission implies in situ particle acceleration up to several TeV. From [17]. Top right: arcmin-scale fossil X-ray jets in the field of 4U 1755-33 [5] (XMM-Newton image). Bottom right: arcsec-scale transient X-ray jet from Circinus X-1 seen with the Chandra gratings. From [53]. The X-ray jet direction coincide with that of the ultra-relativistic radio jets [33].

4 Jet-ISM interaction

4.1 Jet-driven nebulae

It is worth stressing that none of the above scaling relations deals with actual measurements of the *total* jet power, which is a function of the observed radio luminosity, corrected for relativistic effects, and of the unknown radiative efficiency. A fruitful method, borrowed from the AGN community, is that to constrain the jet power×lifetime product by looking at its interaction with the surrounding interstellar medium (ISM). Beside the arcmin-scale, fossil jets around the so called Great Annihilator (Fig. 1, bottom right panel; [99]), a well known case is that of the nebula around the first Galactic jet source discovered: SS 433. The 'ears' of W50 (Fig. 3,

top right panel) act as an effective calorimeter for the jets' mechanical power, which is estimated to be greater than 10^{39} erg s^{-1} [9]. Similarly, the neutron star X-ray binary in Circinus X-1 is embedded in an extended, jet-driven radio nebula (see Fig. 3, top left panel). In this particular case, it is likely that we are actually looking toward the central X-ray binary system through the jet-powered radio lobe, making this the only known case of a Galactic *microblazar*. Results from modeling suggest an age for the nebula of $\lesssim 10^5$ yr and a corresponding time-averaged jet power in excess of 10^{35} erg s^{-1} . During flaring episodes, the instantaneous jet power may reach values of similar magnitude to the X-ray luminosity [119].

More recently, a low surface brightness arc of radio/optical emission has been discovered around Cygnus X-1 [47, 108] (Fig. 3, bottom panels) and interpreted in terms of a shocked compressed hollow sphere of free-free emitting gas driven by an under-luminous synchrotron lobe inflated by the jet of Cygnus X-1. The lack of a visible counter arc is ascribed to the lower interstellar matter density in the opposite direction. In fact, there exist to date relatively few cases where jet-ISM interactions have been directly observed [87]. Carrying the analogy of AGN jet-ISM interactions over to microquasars, it has been argued that microquasars are located, dynamically speaking, in much more tenuous atmospheres. As a consequence, compared to AGN, microquasar jets require particularly dense environments in order to produce visible signs of interaction with the surroundings [54, 57].

4.2 X-ray jets

It is well known that, in AGN, optical and X-ray jets are also frequently seen. With the exception of the large-scale (tens of pc) diffuse X-ray emission detected from the X-ray binary SS 433 with the Einstein Observatory [112], X-ray jets were not seen for Galactic systems prior to the launch of the Chandra X-Ray Observatory in 1999. With a large improvement in angular resolution over previous missions, Chandra detected arcsec-scale ($\sim$0.025 pc) X-ray jets for the first time in SS 433 [75]. This was the first of a number of discoveries.

Perhaps the most extreme case in terms of energetics has been the detection of decelerating arcsec-scale X-ray (and radio) jets in the microquasar XTE J1550-564, a few years after the ejection event [21, 117, 68]. The detection of optically thin synchrotron X-ray emission from discrete ejection events implies in situ particle acceleration up to several TeV, possibly due to interaction of the jets with the interstellar medium. More recently, a similar large scale jet has been reported in H 1743-322 [17] (Fig. 4, left panels). As for XTE J1550-564, the spectral energy distribution of the jets during the decay phase is consistent with a classical synchrotron spectrum of a single electron distribution from radio up to X-rays, implying the production of very high energy (>10 TeV) particles in those jets.

Another interesting example is that of a fossil arcmin-scale X-ray jet seen by the XMM-Newton telescope in the surroundings of 4U 1755-33 [5] (Fig. 4, top right panel). Finally, evidence for a transient X-ray jet has been recently claimed in the neutron star Circinus X-1 during a 50 ks Chandra gratings observation (Fig. 4, bottom right panel), taken during a low flux state [53]. The direction of this X-ray feature is consistent with the direction of the northwestern jet seen in the radio [33], suggesting that it originates either in the jet itself or in the shock that the jet is driving into its environment. The inferred jet kinetic power is significantly larger than the minimum power required for the jet to inflate the large-scale radio nebula.

5 Quiescence (to eject, or not to eject?)

The role of outflows is especially interesting at very low X-ray luminosities, in the so called 'quiescent' regime, i.e. below a few 10^{-5}L$_{\rm Edd}$. Persistent, steady radio counterparts to BHBs appear to survive down to low quiescent X-ray luminosities (as low as $10^{-8.5}$ L$_{\rm Edd}$ [46]), even though sensitivity limitations on current radio telescopes make it extremely difficult to reach the signal-to-noise ratios required to assess their presence for systems further than 2 kpc or so.

In the context of X-ray binaries, as well as super-massive black holes, the term 'jet' is typically used as a synonymous for relativistic outflow of plasma and implies a high degree of collimation. As a matter of fact, high spatial resolution radio observations of BHBs in the hard state have resolved highly collimated structures in two systems only: Cyg X-1 [114] and GRS 1915+105 [25, 42] are both resolved into elongated radio sources on milliarcsec scales – that is tens of A.U. – implying collimation angles smaller than a few degrees on much larger scales than the orbital separation. Both systems display a relatively high X-ray (and radio) luminosity, with GRS 1915+105 being persistently close to the Eddington luminosity [32], and Cyg X-1 displaying a bolometric X-ray luminosity around 2%L$_{\rm Edd}$ [26].

This, however, should not be taken as evidence against collimated jets in low luminosity, quiescent systems: because of sensitivity limitations on current high resolution radio arrays, resolving a radio jet at microJy level simply constitutes an observational challenge. In addition, at such low levels, the radio flux could be easily contaminated by synchrotron emission from the donor star.

In principle, the presence of a collimated outflow can also be inferred by its long-term action on the local interstellar medium, as in the case of the hard state BHBs 1E 1740.7-2942 and GRS 1758-258, both associated with arcmin-scale radio lobes [99, 79]. Further indications can come from the stability in the orientation of the electric vector in the radio polarization maps, as observed in the case of GX 339−4 over a two year period [22]. This constant position angle, being the same as the sky position angle of the large-scale, optically thin radio jet powered by GX 339-4 after its 2002 outburst [48], clearly indicates a favoured ejection axis in the system. However, all three systems emit X-rays at 'intermediate' luminosities (10^{-3}-10^{-2}L$_{\rm Edd}$), and tell us little about outflows from quiescent BHs. On the other hand, failure to image a collimated structure in the hard state of XTE J1118+480 down to a synthesized beam of 0.6×1.0 mas^2 at 8.4 GHz [94] poses a challenge to the collimated jet interpretation, even though XTE J1118+408 was observed at roughly one order of magnitude lower luminosity with respect to e.g. Cyg X-1 (10^{-3} L$_{\rm Edd}$). Under the (naive) assumption that the jet size scales as the radiated power, one could expect the jet of XTE J1118+408 to be roughly ten times smaller than that of Cyg X-1 (which is 2×6 mas^2 at 9 GHz, at about the same distance), i.e. still point-like at Very Long Based Array (VLBA) scales [94].

In fact, [50] have pointed out that long period ($\gtrsim$ 1 day) BHBs undergoing outbursts tend to be associated with spatially resolved optically thin radio ejections, while short period systems would be associated with unresolved, and hence physically smaller, radio ejections. If a common production mechanism is at work in optically thick and optically thin BHB jets, then the above arguments should apply to steady optically thick jets as well, providing an alternative explanation to the unresolved radio emission of XTE J1118+480 (which, with its 4 hr orbital period, is one of the shortest known). By analogy, a bright, long period system, like for

instance V404 Cyg, might be expected to have a more extended optically thick jet. This is further explored in the next Section.

5.1 The brightest: V404 Cyg

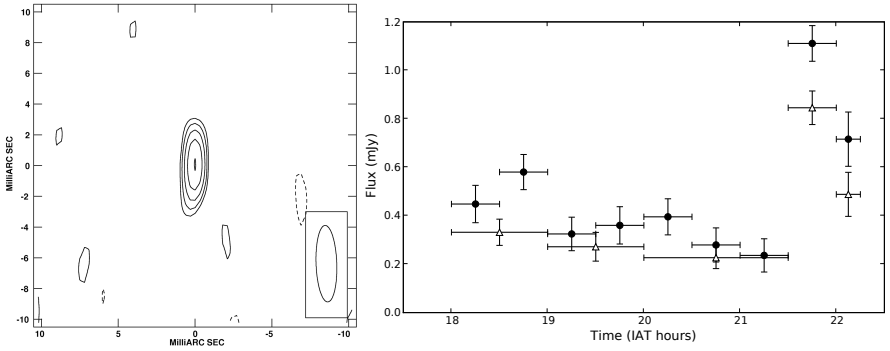

Fig. 5. Left: the quiescent black hole V404 Cyg was observed with the High Sensitivity Array for 4.25 hr at 8.4 GHz. The radio source is unresolved, yielding an upper limit of 5.2 A.U. to the size of the emitting region. Right: the source radio light curve during the observation, showing a flare with 30 min rising time. From [86].

In order to eventually resolve the radio counterpart to a quiescent X-ray binary, the black hole V404 Cyg was observed with the High Sensitivity Array (HSA, composed of: VLBA plus the Green Bank Telescope, Effelsberg and the phased VLA) in 2007 December, for 4.25 hr [86]. These observations failed to resolve the radio source (Fig. 5, left panel), yielding an upper limit of 1.3 milliarcsec on the 8.4 GHz source size – 5.2 A.U. at 4 kpc – and a corresponding lower limit of 7×10^6 K on its brightness temperature (confirming that the radio emission must be non-thermal). Interestingly, the inferred upper limit on the radio source size is already 2 times smaller than the steady jet resolved in Cyg X-1 with the VLBA (Fig. 1, top left panel).

A small flare was detected from V404 Cyg with both the VLA and the VLBA, on a timescale of 1 hr (Fig. 5, right panel), in which the source flux density rose by a factor of 3. As the brightest black hole X-ray binary in quiescence (few 10^{-5} L_{Edd} in X-rays, 0.4 mJy at GHz frequencies), V404 Cyg is the only source in which such flaring activity has been detected in the quiescent state (the flare is certainly intrinsic to the source, and can not be caused by interstellar scintillation [86]). The question of whether flares are unique to this source, or are common in such systems, has direct implications for the nature of the accretion process at low luminosities. Observations of XTE J1118+480 and GX 339-4 in their hard states have shown evidence for fast variability in the optical and X-ray bands [65, 64, 63], with properties inconsistent with X-ray reprocessing and more indicative of synchrotron variability. The timescales are shorter than seen in V404 Cyg, and there were no high-time

resolution radio data for comparison. A better comparison is the quiescent BH in the center of the milky Way, Sgr A*. It shows radio and infrared flaring activity, which has been explained as adiabatic expansion of a self-absorbed transient population of relativistic electrons [121]. Whether there is a truly steady underlying jet as assumed by standard jet models [11, 69] or whether the emission is composed of multiple overlapping flares [70] remains to be determined. More sensitive instruments are necessary to probe these short-timescale ares and determine the nature of the quiescent jet emission (see Sect. 11).

5.2 The faintest: A 0620-00

In spite of the large degree of uncertainty on the overall geometry of the accretion flow in this regime, there is general agreement that the X-ray emission in quiescent BHBs comes from high-energy electrons near the BH. The SEDs of quiescent BHBs, as well as low-luminosity AGN are often examined in the context of the advection-dominated accretion flow (ADAF) solution [103, 102], whereby the low X-ray luminosities are due to a highly reduced radiative efficiency, and most of the liberated accretion power disappears into the horizon. Here, due to the low densities, a two temperature inflow develops, a significant fraction of the viscously dissipated energy remains locked up in the ions as heat, and is advected inward, effectively adding to the BH mass. The ADAF model successfully accounts for the overall shape of the UV-optical-X-ray spectra of quiescent BHBs (see e.g. [81] for an application to the high quality data of XTE J1118+480). Nevertheless, alternative suggestions are worth being considered. [10] elaborated an 'adiabatic inflow-outflow solution' (ADIOS), in which the excess energy and angular momentum is lost to an outflow at all radii; the final accretion rate into the hole may be only a tiny fraction of the mass supply at large radii.

Alternatively, building on the work by [28] on AGN jets, a jet model has been proposed for hard state BHBs [78, 77, 76]. Figure 6, top panel, shows a fit to the radio-to-X-ray SED of A 0620-00, the lowest Eddington-ratio BHB with a detected radio counterpart ($L_X/L_{Edd} \simeq 10^{-8}$; $F_{8\ GHz}$=50 μJy) with such a 'maximally jet-dominated' model [44]. This is the first time that such a complex model was applied in the context of quiescent BHBs, and with the strong constraints on the jet break frequency cut-off provided by the Spitzer Space Telescope data in the mid-IR regime (see Sect. 7 for more details). In terms of best-fitting parameters, the major difference with respect to higher luminosity sources for which this model has been tested [78, 77] (see Chap. 6) is in the value of the acceleration parameter f compared to the local cooling rates, which turns out to be two orders of magnitude lower for A 0620-00. This 'weak acceleration' scenario is reminiscent of the Galactic Center super-massive BH Sgr A*. Within this framework, the SED of Sgr A* does not require a power law of optically thin synchrotron emission after the break from its flat/inverted radio spectrum. Therefore, if the radiating particles have a power-law distribution, it must be so steep as to be indistinguishable from a Maxwellian in the optically thin regime. In this respect, they must be only weakly accelerated. In the framework of a jet-dominated model for the quiescent regime, it appears that something similar, albeit less extreme, is occurring in the quiescent BHB A 0620-00; either scenario implies that acceleration in the jets is inefficient at $10^{-9} - 10^{-8}$ L_{Edd}.

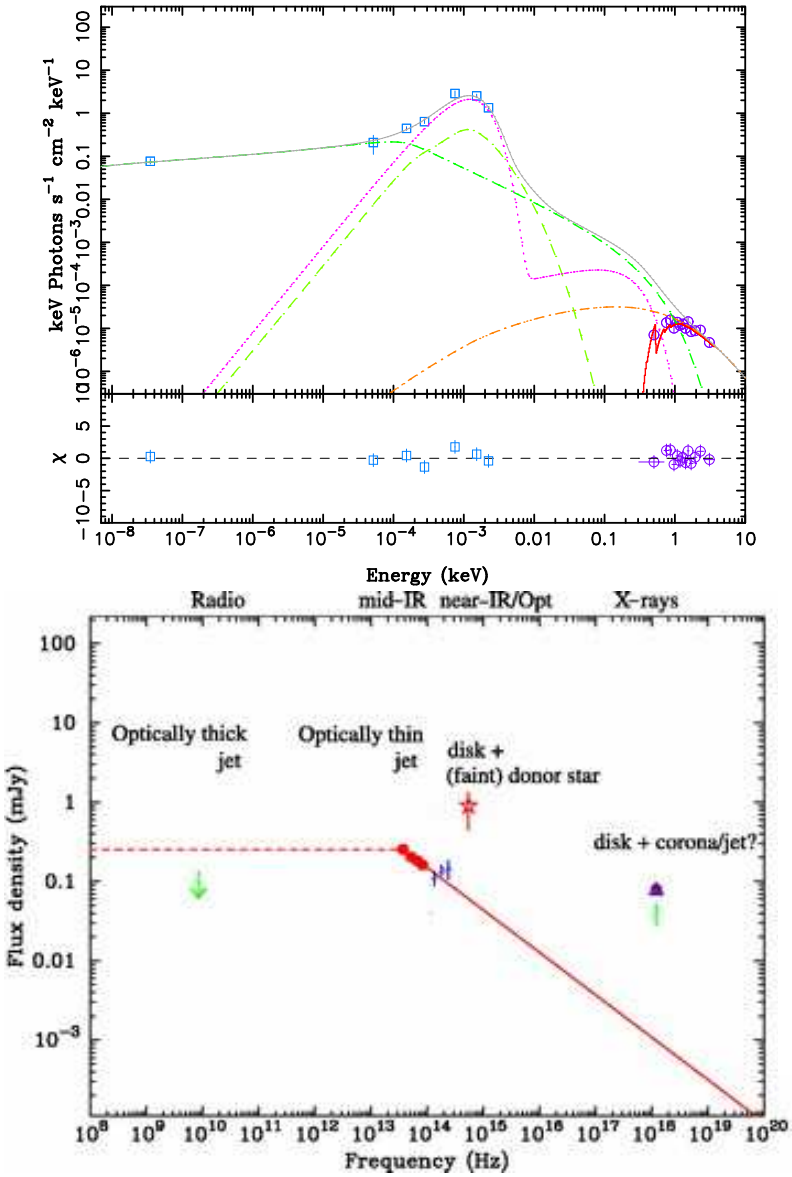

Fig. 6. Top: radio-to-X-ray SED of the quiescent black hole X-ray binary A 0620-00, fit with a 'maximally-dominated' jet model. Solid gray line: total spectrum; dot-long-dashed yellow line: pre-acceleration inner jet synchrotron emission; dotted green line: post-acceleration outer jet synchrotron; triple dot-dashed orange line: Compton emission from the inner jet, including external disk photons as well as synchrotron self-Compton; double-dot-dashed magenta line: thermal multicolor-blackbody disk model plus single blackbody representing the star. The symbols represent the data, while the solid red line is the model fit in detector space. From [44]. Bottom: evidence for optically thin synchrotron emission from a jet in the NS 4U 0614+091. By comparison, if the mid-IR excess detected in the BHs A 0620-00 is indeed due to jet emission, this means that the power content of the BH jet is at least 10 times higher than in the NS, where the jet spectrum breaks to optically thin already at mid-IR frequencies. From [90].

6 Neutron stars

The mechanism(s) of jet production, from an *observational* point of view, remains essentially unconstrained. While in the case of super-massive BHs in AGN it is often implicitly assumed that the jets extract their energy from the rotation of the centrally spinning black hole via large scale magnetic field lines that thread the horizon, in the case of X-ray binaries, the relatively low (lower limit on the) jets' Lorentz factors [35] do not appear to require especially efficient launching mechanisms. While on the 'experimental' side, substantial improvements are being made with fully relativistic magneto-hydrodynamic simulations (e.g. [82], and references therein), from the observer perspective it seems that a fruitful – and yet relatively unexplored – path to pursue is that to compare in a systematic fashion the properties of jets in black hole systems to that of e.g. low magnetic field NSs.

A comprehensive study comparing the radio properties of BHs and NSs [91] has highlighted a number of relevant difference/similarities (see Fig. 7): *i)* Below a few per cent of the Eddington luminosity (in the hard, radiatively inefficient states) both BHs and NSs produce steady compact jets, while transient jets are associated with variable sources/flaring activity at the highest luminosities. *ii)* For a given X-ray luminosity, the NSs are less radio loud, typically by a factor of 30 (Fig. 7, top panel). *iii)* Unlike BHs, NSs do not show a strong suppression of radio emission in the soft/thermal dominant state. *iv)* Hard state NSs seem to exhibit a much steeper correlation between radio and X-ray luminosities.

Highly accreting NSs, called Z-type (Fig. 7, bottom left panel), show periodic X-ray state transitions on timescales of a few days. Z sources can be considered the NS counterparts of transient, strongly accreting BHs such as GRS 1915+105. At the same time, they are known to display hard non-thermal tails in the X-ray energy spectra. The physical origin of this non-thermal component is still an area of controversy, with two main competing models: 1. inverse Compton scattering from a non-thermal electron population in a corona [105], and 2. bulk motion Comptonization [115]. Recently, simultaneous VLA/RXTE observations of the Z source GX 17+2 have shown a positive correlation between the radio emission and the hard tail power-law X-ray flux in this system (Fig. 7, bottom right panel, [89]). If further confirmed with a larger sample and improved statistics, this relation would point to a common mechanism for the production of the jet and hard X-ray tails.

7 Jet power: the mid-IR leverage

Observations of hard state BHBs have established that synchrotron emission from the steady jets extends all the way from the radio to the mm-band [40], above which the break to the optically thin portion of the spectrum is thought to occur. However, even for the highest quality SED, disentangling the relative contributions of inflow vs. outflow to the radiation spectrum and global accretion energy budget can be quite challenging, as exemplified by the emblematic case of XTE J1118+480 [81, 77, 122]. Estimates of the total jet power based on its radiation spectrum depend crucially on the assumed frequency at which the flat, partially self-absorbed spectrum turns and becomes optically thin, as the jet 'radiative efficiency' depends ultimately on

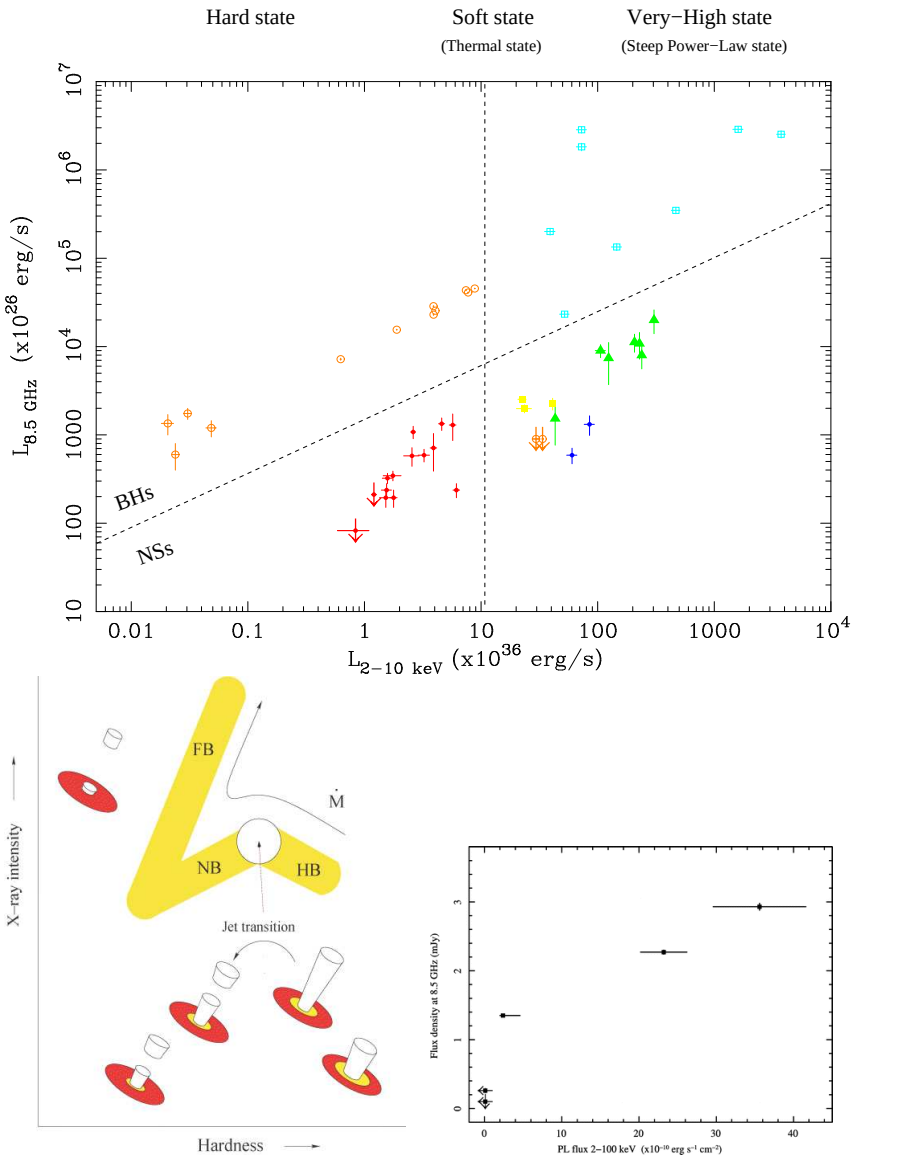

Fig. 7. Top: radio vs. X-ray luminosity for (2 representative) black holes (top left) and neutron stars (bottom right). On average, neutron stars are 30 times fainter in the radio band. From [91]. Bottom left: sketch of the disk-jet coupling in Z-type sources, which are believed to be the NS equivalents of the BH GRS 1915+105, constantly emitting near L_{Edd} and producing powerful jets associated with rapid state transitions. From [91]. Bottom right: a correlation between the core radio flux density and the X-ray flux in the hard X-ray in the Z source GX 17+2. From [89].

the location of the high-energy cutoff induced by the higher synchrotron cooling rate of the most energetic particles. From a theoretical point of view, the 'break frequency', here defined as the frequency at which the partially self-absorbed jet becomes optically thin, is inversely proportional to the BH mass: as jet spectral breaks are often observed in the GHz/sub-mm regime in AGN, they are expected to occur in the IR-optical band for 10^{5-7} times lighter objects. We know however from observations of GX 339-4, the only BHB where the optically thin jet spectrum has been perhaps observed [20, 61], that the exact break frequency can vary with the overall luminosity, possibly reflecting changes in the magnetic field energy density, particle density and mass loading at the jet base. Determining the location of the jet break as a function of the bolometric luminosity is also important to assess the synchrotron contribution to the hard X-ray band. As an example, that the optically thin jet IR-emission in GX 339-4 connects smoothly with the hard X-ray power law has led to challenge the 'standard' Comptonization scenario for the hard X-ray state [77].

Because of the low flux levels expected from the jets in this regime (10–100s of μJy, based on extrapolation from the radio band), combined with the companion star/outer disk contamination at near-IR frequencies, the sensitivity and leverage offered by Spitzer is crucial in order to determine the location of the jet break. In fact, Spitzer observations of three quiescent black hole X-ray binaries, with the Multi-band Imaging Photometer (MIPS), have shown evidence for excess emission with respect to the Rayleigh-Jeans tail of the companion star between 8–24 μm. This excess, which has been interpreted as due to thermal emission from cool circumbinary material [100], is also consistent with the extrapolation of the measured radio flux assuming a slightly inverted spectrum, typical of partially self-absorbed synchrotron emission from a conical jet [44]. If so, then the jet synchrotron luminosity exceeds the measured X-ray luminosity by a factor of a few in these systems. Accordingly, the mechanical power stored in the jet exceeds the bolometric X-ray luminosity at least by 4 orders of magnitude (based on kinetic luminosity function of Galactic X-ray binary jets [55]).

Despite their relative faintness with respect to BHs at low (radio) frequencies, the same multi-wavelength approach can be undertaken in NSs, in the hope to detect excess mid-IR emission. Indeed, coordinated radio (VLA), mid-IT (Spitzer), optical (YALO SMARTS) and X-ray (RXTE) observations, have yielded the first spectroscopical evidence for the presence of a steady jet in a low-luminosity, ultra-compact[1] neutron star X-ray binary (4U 0614+091 [90]). The Spitzer data (Fig. 6, bottom panel) show a neat optically *thin* synchrotron spectrum ($F_\nu \propto \nu^{-0.6}$), indicating that the jet break occurs at much lower frequencies in this neutron star system with respect to black hole X-ray binaries. As a consequence, unlike in the black holes, the jet can not possibly contribute significantly to the X-ray emission.

The Spitzer results on low-luminosity X-ray binaries (3 BHs and 1 NS; [90, 44]) seem to point towards different energy dissipation channels in different classes of objects, namely: the former seem to be more efficient at powering synchrotron emitting outflows, having partially self-absorbed jets which extend their spectrum up to the near-IR band. However, it is worth reminding that the most relativistic jet

[1] That is, with orbital period shorter than 1 hour.

discovered in the Galaxy so far, is that the neutron star X-ray binary Circinus X-1 [33], for which the inferred Lorentz factor exceeds 15 (see Fig. 8).

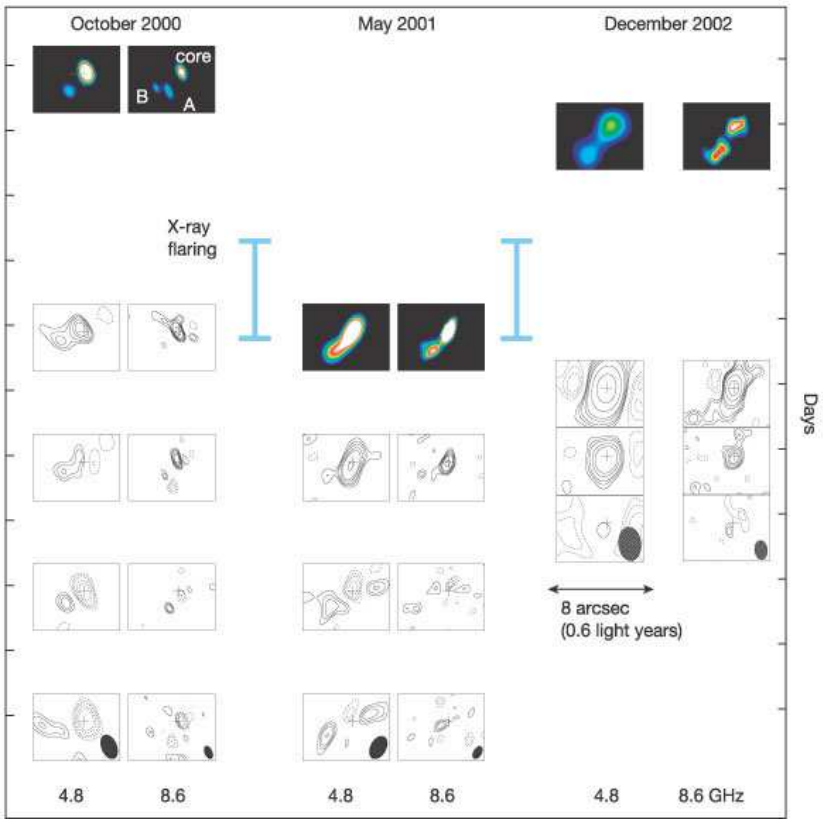

Fig. 8. An ultra-relativistic jet powered by the neutron star X-ray binary Circinus X-1. From [33]. The inferred bulk Lorentz factor exceeds $\Gamma = 15$, making this the most relativistic Galactic jet source to date.

8 Jets, advection and event horizon

One of the most cited accomplishments of the ADAF model is to naturally account for the relative dimness of quiescent BHBs with respect to quiescent NS X-ray binaries [101]: whereas in the case of a BH accretor all the advected energy disappears as it crosses the horizon, adding to the BH mass, the same energy is released and radiated away upon impact in the case of an accretor with solid surface. Under the ADAF working-hypothesis, such luminosity difference – which is indeed observed in X-rays [51] – is actually taken as observational evidence for the existence of an horizon in BHBs.

However, while the observed luminosity gap may well be a natural byproduct of advection of energy through the BH horizon, the possibility exists that the very mechanism of jet production differs between the two classes, and that the observed luminosity difference is due to different channels for dissipating a common energy reservoir, with the black hole 'preferring' jets (as discussed in Sect. 6, the NSs are indeed fainter than the BHs in the radio band).

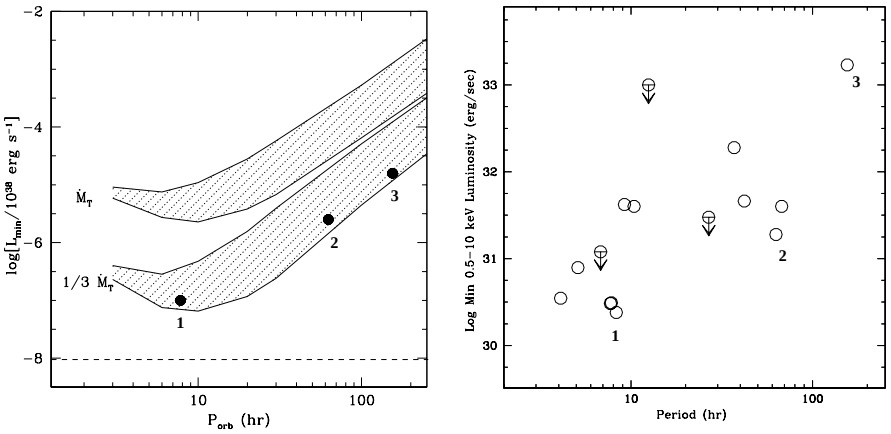

Fig. 9. Left: in the ADAF scenario, the minimum luminosity around a few 10^{30} erg s^{-1} corresponds to roughly 2/3 of the outer accretion rate lost to a wind/outflow. From [83]. Right: quiescent X-ray luminosities/upper limits for 15 BH X-ray binaries, plotted against the systems' orbital periods. From [43].

Out of 15 BHB systems with sensitive X-ray observations while in the quiescent regime, 12 have now been detected in X-rays (see Fig. 9, right panel; updated from [118] after [18, 46, 59]). For those 12, the quiescent luminosities range between a few 10^{30} and 10^{33} erg s^{-1} . The nearest BH, A 0620-00, has been steadily emitting at $\simeq 2-3\times10^{30}$ erg s^{-1} at least for the past 5 years [46]; this is approximately the same luminosity level as XTE J1650-500 [43], XTE J1118+480 [81] and GS 2000+25 [51], suggesting that this might be some kind of limiting value.

In fact, for low-mass X-ray binaries one can make use of binary evolution theory, combined with a given accretion flow solution, to predict a relation between the minimum quiescent luminosity and the system orbital period, $P_{\rm orb}$ [83, 66]. Independently of the actual solution for the accretion flow in quiescence, the existence of a minimum luminosity in low-mass X-ray binaries stems directly from the existence of a bifurcation period, $P_{\rm bif}$, below which the mass transfer rate is driven by gravitational wave radiation (j-driven systems), and above which it is dominated by the nuclear evolution of the secondary star (n-driven systems). As long as the luminosity expected from a given accretion flow model scales with a positive power of the outer accretion rate, systems with orbital periods close to the bifurcation period should display the lowest quiescent luminosity. As an example, the left panel of Fig. 9 (from [83]) illustrates how the predicted luminosity of quiescent BHs pow-

ered by ADAFs depends on the ratio between the outer mass transfer rate and the ADAF accretion rate. The lower band for instance corresponds to $\sim 1/3$ of the outer mass transfer being accreted via the ADAF, implying that the remaining 2/3 is lost to an outflow (effectively making this inflow an ADIOS [10]). Interestingly, this lower band roughly reproduces the observed luminosities of 3 representative systems spanning the whole range of detected systems (1. A 0620-00, 2. GRO J1655-40 and 3. V404 Cyg – marked in both panels).

9 White Dwarfs

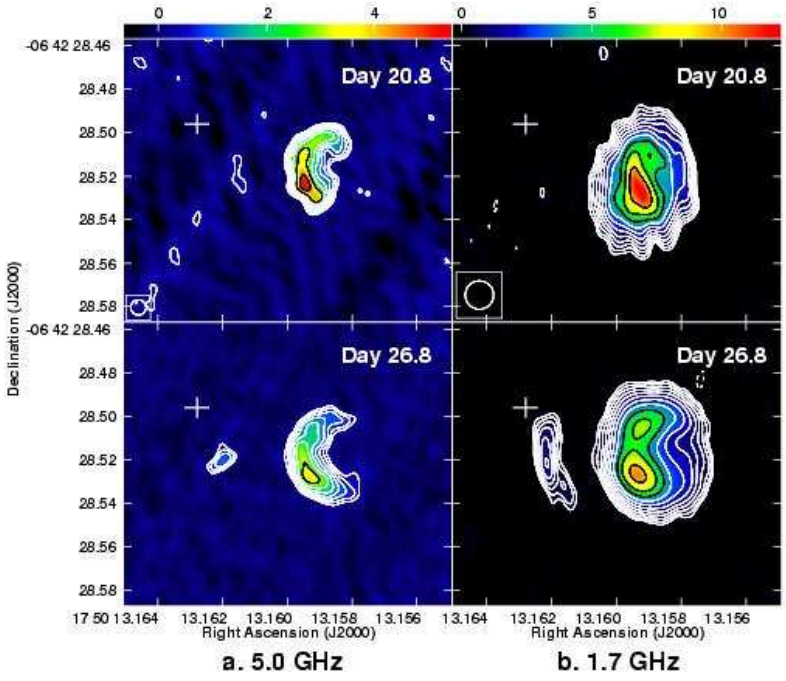

Fig. 10. Two epoch, post-outburst, radio observations of the recurrent nova RS Ophiuchi (VLBA). The second epoch observations (bottom) show evidence for an additional resolved component to the east of the shell-like feature visible already in the first epoch (top). From [107].

Accreting WDs come in three main classes: cataclysmic variables (CVs), supersoft X-ray binaries, and symbiotic stars. Perhaps the best-understood of all accretion disks are those in cataclysmic variables (CVs). Although outflows have been observed

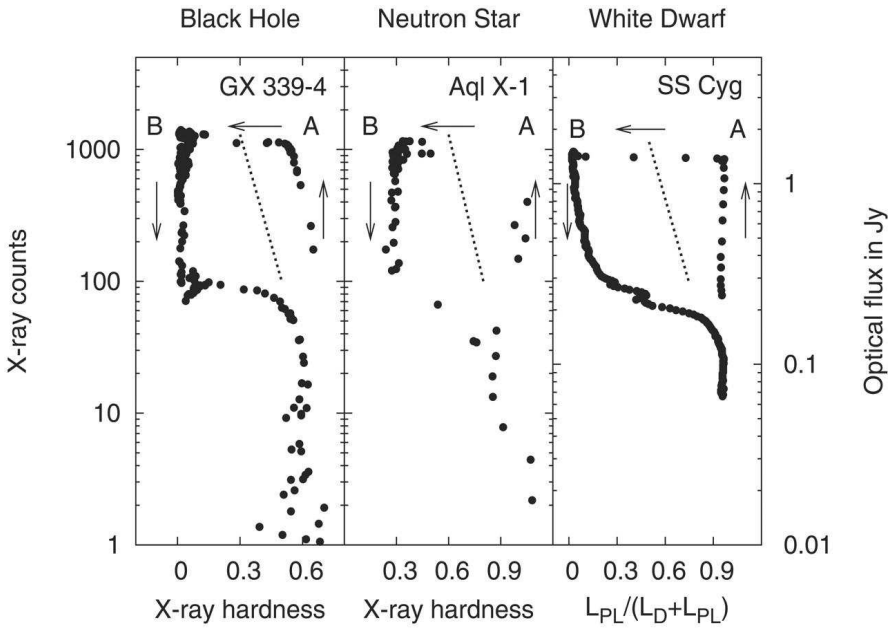

Fig. 11. Disk-fraction vs. luminosity diagrams for Galactic binary stellar systems and microquasar sources hosting different compact objects: a BH, NS and WD. From [72]. This study provides the strongest observational evidence to date for a synchrotron-emitting outflow from a dwarf nova system, and strengthens the similarities between jet sources across the whole mass spectrum.

from an increasing number of accreting WDs in symbiotic stars and supersoft X-ray sources [113, 71], these are generally not spatially well resolved, and questions on the jet-accretion coupling remain open. Most WD ejecta have velocities of hundreds to thousands of km s^{-1}, and even in those cases when the emission can be spatially separated from the binary core, it usually appears to be due to free-free emission from shocks. However, a handful of observations suggests that the outflowing particles can be accelerated to high enough energies that non-thermal radio and/or X-ray emission can also be produced [23, 104].

Two recent works [107, 72] have provided us with the best observational evidence for synchrotron emission from a WD jet. As illustrated in Fig. 10, VLBA observations of the recurrent nova RS Ophiuchi, taken about 21 and 27 days after the outburst peak, have imaged a resolved synchrotron component well to the east of the shell-like shock feature[2]. Interestingly, the inferred jet velocity is comparable to the escape velocity from a WD.

A second example is the detection of a transient radio jet erupting from the dwarf nova SS Cyg [72]. Radio observations of this system, conducted during its

[2] Typically, post-outburst radio emission from RS Ophiuchi originates from dense ISM that is swept up, compressed and shocked by the relatively rarefied shell that has been ejected [111]

2007 April outburst with the VLA, revealed a variable, flat-spectrum source with high brightness temperature, most likely due to partially self-absorbed synchrotron emission from a jet [72]. As apparent from Fig. 11, the behavior of SS Cyg (right panel) during the outburst closely resembles that of X-ray binaries hosting relativistic compact objects. Plotted here, from left to right, are the 'disk-fraction vs. luminosity diagrams' (which can be seen as the generalization of HIDs generally adopted for X-ray binaries; see [73]) for three different accreting objects: a BH, NS and the WD SS Cyg. Unlike for BHs and NSs, where the x-axis is the X-ray spectral hardness, for the WD case this variable has been replaced by the power-law fraction, which quantifies the prominence of the power law component over the boundary layer/thermal disk component of the energy spectrum, as measured in the optical/UV band. Evidently, the three systems occupy the same region of the parameter space during a typical outburst (see Fig. 2 for a schematic of typical BH outburst HID, and Fig. 7, bottom left panel, for Z-type NSs), the most notable difference being that – for the BHs – the core, flat spectrum radio emission drops below detectable levels when in the soft/thermal dominant state, while it seems to be only somewhat weakened in NSs and WDs.

These results provide further support to the hypothesis that the mere existence of accretion coupled to magnetic fields may be sufficient ingredients for a jet to form, independently of the presence/absence of an horizon. However, the latter (or, put it another way, the presence of a physical surface) could play a role in: *i)* making the jets more radio loud; *ii)* enhancing the magnitude of the jet suppression mechanism during bright soft states.

10 Jet production, collimation, matter content

It is often assumed that the velocity the the steady jet is only mildly relativistic, with $\Gamma \simeq 2$ [49]. This comes from the relative spread about the radio/X-ray correlation, interpreted as evidence for a low average Lorentz factor. However, this argument has been confuted on theoretical grounds [56]. As far as the transient jets are concerned, there is a high degree of uncertainties in estimating their Lorentz factors, mainly because of distance uncertainties [35].

A recent work [88] made a substantial step forward in constraining the Lorentz factor of microquasars by means of the observational upper limits on the jets' opening angles. This method relies on the fact that, while the jets could undergo transverse expansion at a significant fraction of the speed of light, time dilation effects associated with the bulk motion will reduce their apparent opening angles. [88] have calculated the Lorentz factors required to reproduce the small opening angles that are observed in most X-ray binaries, with very few exceptions, under the crucial assumption of no confinement. The derived values, mostly lower limits, are larger than typically assumed, with a mean $\Gamma_{\rm m} > 10$. No systematic difference appears to emerge between hard state steady jets and transient plasmons (Fig. 12). If indeed the transient jets were as relativistic as the steady jets, as already mentioned, this would challenge the hypothesis of internal shocks at work during hard-to-thermal state transitions in BHBs. In order for that scenario to be viable, the transient jets must have higher Lorentz factor; in other words, steady jets ought to be laterally confined.

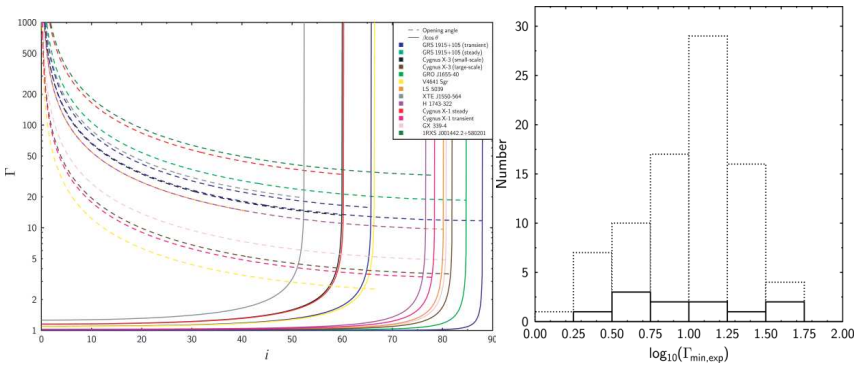

Fig. 12. Left: Lorentz factors derived from opening angles (Eq. 4 in [88], dashed lines) and from the inferred $\beta \times \cos i$ products for a number of microquasars. Since the Lorentz factors are derived from upper limits on the opening angles they are in fact lower limits (assuming freely-expanding jets with an expansion speed c). Right: Mean Lorentz factors for X-ray binaries from opening angles' constraints (solid), compared to AGN from proper motions' (dashed). From [88].

The issue of the jets' matter content remains highly debated. Perhaps with the exception of SS 433 [120, 92], where atomic lines have been detected at optical at X-ray wavelengths along the jets (see Fig. 13), various studies come to different conclusions for different sources. For example, circular polarization, which in principle can provide an excellent tool for investigating the baryonic content of the jets, is only detected in a handful of sources [38], where no strong conclusion could be placed yet. Entirely different studies (e.g. based on modeling large scale jet-ISM interaction structures by means of self-similar jet fluid models) also draw different conclusions: in the case of Cygnus X-1 for instance, some authors [47, 54] argue for cold baryons in the flow, while an electron/positron jet seems to be favored in GRS 1915+105 based on energetics arguments [38].

11 Future prospects

In this last Section, I choose to briefly introduce a number of observational capabilities that are about to become available to the community – or have just started to – that I believe will literally revolutionize our understanding of microquasars (and not only).

11.1 Next generation radio interferometers

With an imaging resolution of 50 milliarcsec at 40 GHz, the imaging capability of the VLA is comparable with the highest resolution of Advanced Camera for Surveys on-board the Hubble Space Telescope. However, the fundamental data-processing capabilities of the VLA remained essentially unchanged since the 70s'. The Expanded

VLA (EVLA[3]) will dramatically improve its ability to make high-sensitivity and high-resolution images. The EVLA will attain unprecedented image quality with 10 times the sensitivity and 1000 times the spectroscopic capability of the existing array. Finally, the addition of eight new antennas will provide an order-of-magnitude increase in angular resolution. At the time of writing, the number of EVLA antennas continues to increase at a rate of one every two months. Each upgraded EVLA antenna produces 100 times more data than an original VLA antenna. When completed in 2012, the EVLA will be the most powerful centimeter-wavelength radio telescope in the world. The technology developed for the EVLA will enable progress on the next generation radio telescope: the Square Kilometer Array.

With baselines of up to 217 km, the Multi-Element Radio Linked Interferometer Network (MERLIN) provides cm-wavelength imaging at 10 to 150 milliarcsec resolution, effectively covering the gap between arrays such as the Westerbork Synthesis Radio Telescope (WSRT) and the VLA, and Very Long Based Interferometry (VLBI) arrays such as the VLBA and the European VLBI Network (EVN). e-MERLIN[4] is a major UK project aimed at increasing the bandwidth and thus the sensitivity of MERLIN by about an order of magnitude. This increased sensitivity, together with the high resolution provided by the long baselines, will enable a wide range of new astronomical observations, including of course Galactic microquasars. One other major development which is part of the upgrade is frequency flexibility, as e-MERLIN will be able to switch rapidly between 1.4, 5, 6 and 22 GHz. The e-MERLIN telescope array is now nearing completion, and will soon start to acquire data for its approved legacy programs.

In terms of microquasar studies, the EVLA and e-MERLIN will be simply a revolution. They will allow for the detection of faint quiescent systems in short exposures, enabling us to test whether collimated jets survive in quiescent black holes (such as V404 Cyg). It will be possible to perform systematic searches for radio counterparts to NSs. Radio outbursts will hopefully receive the same daily coverage as X-rays outbursts do, and with amazingly fast frequency switching capabilities. Deep searched for low surface brightness jet-powered nebulae will be carried out at relatively (comparatively) limited expenses in terms of telescope time. Finally, we will be able to perform spectroscopic studies of microquasars jet, search for lines, possibly constrain the jet baryon content *directly*.

LOFAR[5] (Low Frequency Array) is a next-generation radio telescope currently under construction in The Netherlands, with baseline stations under development over a number of EU countries. The array will operate in the 30-80 and 120-240 MHz bands, thus representing the largest of the pathfinders for the lowest-frequency component of the Square Kilometer Array (SKA) project (see [29]). Core Station One of LOFAR is currently operating; according to the plan, 36 stations will be deployed by the end of 2009.

LOFAR will literally revolutionize the study of bursting and transient radio phenomena at low radio frequencies. So far, the primary instruments for detecting extragalactic Gamma-ray bursts and galactic microquasars have been orbiting satellites, such as BeppoSAX, INTEGRAL, RXTE, Swift and others. One of the break-

[3] `http://www.aoc.nrao.edu/evla/`

[4] `http://www.jb.man.ac.uk/research/rflabs/eMERLIN.html`

[5] `http://www.lofar.org/`

throughs in this field was the localization of Gamma-ray burst and their subsequent identification with supernovae/galaxies at high red-shifts. From the empirical relation between radio and X-ray emission for these systems (see Chap. 5) it is apparent that the all-sky monitoring with LOFAR will be a factor of 5-10 more effective in discovering such events than previous all-sky-monitors [29]. Furthermore, LOFAR will allow much more accurate localization of these events, enabling fast response science and follow-ups at other wavelengths.

11.2 γ-ray binaries

A new observational window has just been opened by ground-based Cherenkov telescopes, HESS[6] (High Energy Stereoscopic System) and MAGIC[7] (Major Atmospheric Gamma-ray Imaging Telescope), that survey the sky above 100 GeV. Because of their high sensitivity, and high angular and energy resolution, these telescopes are revealing and identifying a plethora of new extragalactic and galactic sources of very-high energy (>100 GeV) radiation. The Galactic Center, supernovae remnants, pulsar-wind nebulae, and some 'γ-ray binaries' have all been identified

[6] `http://www.mpi-hd.mpg.de/hfm/HESS/HESS.html`
[7] `http://wwwmagic.mppmu.mpg.de/`

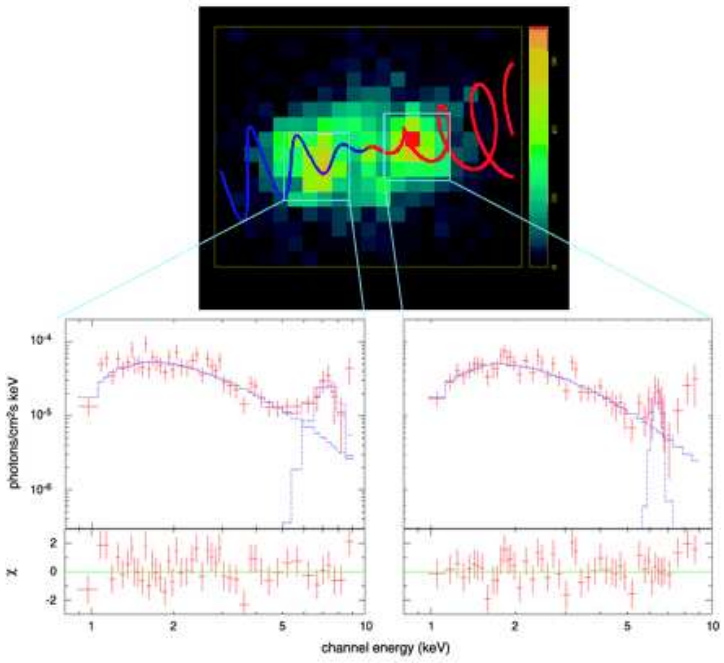

Fig. 13. Chandra image of SS 433 with the projected precession cycle of the jets superimposed on it. These observations reveal evidence for a hot continuum and Doppler-shifted iron emission lines from spatially resolved regions. From [92].

as very high γ-ray sources in the Galaxy [93]. The HESS collaboration reported the detection of TeV γ-ray emission from the Be type binary system PSR B1259-63, close to the periastron passage [1]. Also TeV γ-rays have been detected from LS 5039 [2] and LS I +61 303 [4]. The idea of Galactic jet sources as capable of accelerating particles up to very high energies has been strengthened by the direct detection of large scale X-ray jets resulting from in-situ shocks where electrons are accelerated up to TeV energies [21, 17]. The synergy between very high energies and lower frequency observations is exemplified by the recent detection of a γ-ray flare from the BH X-ray binary Cygnus X-1, reported by the MAGIC collaboration. The flare, seen simultaneously with RXTE, Swift, and INTEGRAL, was compatible with a point-like source at a position consistent with the binary system, thus ruling out its arcmin scale jet-driven radio nebula [3]. Alternatively, relativistic particles can be injected in the surrounding medium by the wind from a young pulsar (see e.g. the case of LS I +61 303 [24]). Coordinated multi-wavelength monitoring can discriminate between competing models, as they predict different emission regions for the radio and γ-ray radiation (core vs. arc-minute scale γ emission can now be resolved by high resolution γ-ray facilities), as well as different flux variations with the orbital phase.

Finally, scheduled to launch in mid 2008, the Gamma-ray Large Area Space Telescope[8] (GLAST) is an international and multi-agency space mission which will study the cosmos in the energy range 10 keV - 300 GeV, complementing ground-based Cherenkov telescopes with wider field. In the 90s, EGRET (the Energetic Gamma Ray Experiment Telescope) made the first complete survey of the sky in the 30 MeV–10 GeV range, showing the γ-ray sky to be surprisingly dynamic and diverse. *Most* of the EGRET sources remain unidentified (170 over 271): this outlines the importance and potentials for new discoveries of the GLAST mission, whose Large Area Telescope (LAT) has a field of view about twice as wide (more than 2.5 steradians), and sensitivity about 50 times at 100 MeV.

The future is bright.

Acknowledgments: The author is supported by NASA through a Hubble Fellowship grant HST-HF-01218 issued from the Space Telescope Science Institute, which is operated by the Association of Universities for Research in Astronomy, Incorporated, under NASA contract NAS5-26555. I wish to thank Rob Fender, Elmar Körding, James Miller-Jones and Valeriu Tudose for providing me with original figures, in part still unpublished.

References

1. F. Aharonian, A. G. Akhperjanian, K.-M. Aye et al.: A&A **442**, 1 (2005a)
2. F. Aharonian, A. G. Akhperjanian, K.-M. Aye et al.: Science **309**, 746 (2005b)
3. J. Albert, E. Aliu, H. Anderhub et al.: ApJ **665**, L51 (2007)
4. J. Albert, E. Aliu, H. Anderhub et al.: Science **312**, 1771 (2006)
5. L. Angelini, N. E. White: ApJ **586**, L71 (2003)
6. T. M. Belloni, I. Parolin, M. Del Santo et al.: MNRAS **367**, 1113 (2006)
7. T. M. Belloni, M. Méndez, A. R. King A. R. et al.: ApJ **488**, L109 (1997)

[8] `http://glast.gsfc.nasa.gov/`

8. T. M. Belloni, M. Méndez, M., A. R. King et al.: ApJ **479**, L145 (1997)
9. M. C. Begelman, A. R. King, J. E. Pringle: MNRAS **370**, 399 (1980)
10. R. D. Blandford, M. C. Begelman: MNRAS **303**, L1 (1999)
11. R. D. Blandford, A. Königl: ApJ **232**, 34 (1979)
12. K. Blundell, M. G. Bowler: ApJ **616** L159 (2004)
13. C. Brocksopp, S. Corbel, R. P. Fender et al.: MNRAS **356**, 125 (2005)
14. C. Brocksopp, R. P. Fender, M. McCollough et al.: MNRAS **331**, 765 (2002)
15. M. Cadolle-Bel, M. Ribó, J. Rodriguez et al.: ApJ **659**, 549 (2007)
16. S. Chaty: Multi-wavelength observations of the microquasar XTE J1720-318: a transition from high-soft to low-hard state. In: *Proceedings of the VI Microquasar Workshop: Microquasars and beyond* ed by T. Belloni (Proceedings of Science) p. 141 (2007)
17. S. Corbel, P. Kaaret, R. P. Fender et al.: ApJ **632**, 504 (2005)
18. S. Corbel, R. P. Fender, J. A. Tomsick et al.: ApJ **617**, 1272 (2004)
19. S. Corbel, M. Nowak, R. P. Fender et al.: A&A **400**, 1007 (2003)
20. S. Corbel, R. P. Fender: ApJ **573**, L35 (2002)
21. S. Corbel, R. P. Fender, A. K. Tzioumis et al.: Science **298**, 196 (2002)
22. S. Corbel, R. P. Fender, A. K. Tzioumis et al.: A&A **359**, 251 (2000)
23. M. M. Crocker, R. J. Davis, S. P. S. Eyres et al.: MNRAS **326**, 781 (2001)
24. V. Dhawan, A. Mioduszewski, M. Rupen: LS I +61 303 is a Be-Pulsar binary, not a Microquasar. In: *Proceedings of the VI Microquasar Workshop: Microquasars and beyond* ed by T. Belloni (Proceedings of Science) p. 52 (2007)
25. V. Dhawan, I. F. Mirabel, L. F. Rodríguez: ApJ **543**, 373 (2000)
26. T. Di Salvo, C. Done, P. T. Zycki et al.ApJ **547**, 1024 (2001)
27. G. M. Dubner, M. Holdaway, W. M. Goss et al.: Astron. J. **116**, 1842 (1998)
28. H. Falcke, P. L. Biermann: A&A **293**, 665 (1995)
29. R. P. Fender: LOFAR Transients and the Radio Sky Monitor. In *Bursts, Pulses and Flickering: wide-field monitoring of the dynamic radio sky.* ed by A. Tzioumis, Lazio and R. Fender (Proceedings of Science) (2008) [arXiv0805.4349]
30. R. P. Fender: Radio emission and jets from X-ray binaries. In: *Compact Stellar X-Ray Sources*, ed by W. H. G. Lewin, M. van der Klis (Cambridge University Press 2006)
31. R. P. Fender, A. M. Stirling, R. E. Spencer et al.: MNRAS **369**, 603 (2006)
32. R. P. Fender, T. M. Belloni: ARA&A **42**, 317 (2004)
33. R. P. Fender, K. Wu, H. Johnston et al.: Nature **427**, 222 (2004)
34. R. P. Fender, T. M. Belloni, E. Gallo: MNRAS **355**, 1105 (2004)
35. R. P. Fender: MNRAS **340**, 1353 (2003)
36. R. P. Fender: ARA&A **288**, 79 (2003)
37. R. P. Fender, E. Gallo, P. G. Jonker: MNRAS **343**, L99 (2003)
38. R. P. Fender, D. Rayner, S. A. Trushkin et al.: MNRAS **330**, 212 (2002)
39. R. P. Fender: MNRAS **322**, 31 (2001)
40. R. P. Fender, R. M. Hjellming, R. P. J. Tilanus: MNRAS **322**, L23 (2001)
41. R. P. Fender, S. Corbel, A. K. Tzioumis et al.: ApJ **519**, L165 (1999)
42. Y. Fuchs, J. Rodriguez, I. F. Mirabel et al.: A&A **409**, L35 (2003)
43. E. Gallo, J. Homan, P. G. Jonker et al.: (2008) ApJ, submitted
44. E. Gallo, S. Migliari, S. Markoff et al.: MNRAS **670**, 600 (2007)
45. E. Gallo: Astrophys. & Space Science **311**, 161 (2007)
46. E. Gallo, R. P. Fender, J. C. A. Miller-Jones et al.: MNRAS **370**, 1351 (2006)
47. E. Gallo, R. P. Fender, C. Kaiser et al.: Nature **436**, 819 (2005)

48. E. Gallo, S. Corbel, R. P. Fender et al.: MNRAS **347**, L52 (2004)
49. E. Gallo, R. P. Fender, G. G. Pooley: MNRAS **344**, 60 (2003)
50. M. R. Garcia, J. M. Miller, J. E. McClintock et al.: ApJ **591**, 388 (2003)
51. M. R. Garcia, J. E. McClintock, R. Narayan et al.: ApJ **553**, L47 (2001)
52. B. Hiemstra, P. Soleri, M. Mendez et al.: MNRAS, in press (arXiv:0901.2255)
53. S. Heinz, N. S. Schulz, W. N. Brandt et al.: ApJ **663**, L93 (2007)
54. S. Heinz: ApJ **636**, 316 (2006)
55. S. Heinz, H. J. Grimm: MNRAS **633**, 384 (2005)
56. S. Heinz, A. Merloni: MNRAS **355**, L1 (2004)
57. S. Heinz: New Astron. Rev. **47**, 565, (2003)
58. R. M. Hjellming, K. J. Johnston: ApJ **328**, 600 (1988)
59. J. Homan, R. Wijnands, A. Kong et al.: MNRAS **366**, 235 (2006)
60. J. Homan, T. M. Belloni: Astrophys. & Space Science **300**, 107 (2005)
61. J. Homan, M. Buxton, S. Markoff et al.: ApJ **624**, 295 (2005)
62. J. Homan, R. Wijnands, M. van der Klis et al.: ApJ **132**, 377 (2001)
63. R. I. Hynes, P. A. Charles, R. M. Garcia et al.: ApJ **611**, L125 (2004)
64. R. I. Hynes, C. A. Haswell, W. Cui et al.: MNRAS **345**, 292 (2003)
65. R. I. Hynes, C. A. Haswell, S. Chaty et al.: ApJ **539**, L37 (2000)
66. J.-P. Lasota: Comptes Rendus Physique **8**, 45 (2007)
67. B. F. Liu, R. E. Taam, E. Meyer-Hofmeister et al.: ApJ **671**, 695 (2007)
68. P. Kaaret, S. Corbel, J. A. Tomsick et al.: ApJ **582**, 945 (2003)
69. C. R. Kaiser: MNRAS **367**, 1083 (2006)
70. C. R. Kaiser, R. Sunyaev, H. C. Spruit: A&A, **356**, 975 (2001)
71. K. S. Kawabata, Y. Ohyama, N. Ebizuka et al.: AJ **132**, 433 (2006)
72. E. Körding, M. Rupen, C. Knigge et al.: Science **320**, 1318 (2008)
73. E. Körding, S. Jester, R. Fender: Mon. Not. R. Astron. Soc. **372**, 1366 (2006).
74. E. Körding, R. P. Fender, S. Migliari: MNRAS **369**, 1451 (2006)
75. H. L. Marshall, C. R. Canizares, N. S. Schulz: ApJ **564**, 941 (2002)
76. S. Markoff, M. A. Nowak, J. Wilms: ApJ **635**, 1203 (2005)
77. S. Markoff, H. Falcke, R. P. Fender: A&A **397**, 645 (2003)
78. S. Markoff, H. Falcke, R. P. Fender: A&A **372**, L25 (2001)
79. J. Martí, S. Mereghetti, S. Chaty et al.: A&A **338**, L95 (1998)
80. J. E. McClintock, R. A. Remillard: Black hole binaries. In: *Compact Stellar X-Ray Sources*, ed by W. H. G. Lewin, M. van der Klis (Cambridge University Press 2006)
81. J. E. McClintock, R. Narayan, M. R. Garcia et al.: ApJ **593**, 435 (2003)
82. J. C. McKinney: MNRAS **368**, 1561 (2006)
83. K. Menou, A. A. Esin, R. Narayan et al.: ApJ **520**, 276 (1999)
84. J. M. Miller, J. Homan, G. Miniutti: ApJ **652**, L113 (2006)
85. J. M. Miller J. Homan, D. Steeghs et al.: ApJ **653**, 525 (2006)
86. J. C. A. Miller-Jones, E. Gallo, M. Rupen et al.: MNRAS in press (2008) [arXiv:0805.4603]
87. J. C. A. Miller-Jones, C. R. Kaiser, T. J. Maccarone et al.: Searching for the signatures of jet-ISM interactions in X-ray binaries. In *Proceedings of A Population Explosion: The Nature and Evolution of X-ray Binaries in Diverse Environments*, ed by M. Bandyopadhyay, S. Wachter, D. Gelino, C. R. Gelino (2008) [arXiv:0802.3446]
88. J. C. A. Miller-Jones, R. P. Fender, E. Nakar: MNRAS **367**, 1432 (2006)
89. S. Migliari, J. C. A. Miller-Jones, R. P. Fender et al.: ApJ **671**, 706 (2007)

90. S. Migliari, J. A. Tomsick, T. J. Maccarone et al.: ApJ **643**, L41 (2006)
91. S. Migliari, R. P. Fender: MNRAS **366**, 79 (2006)
92. S. Migliari, R. P. Fender, M. Méndez: Science **297**, 1673 (2002)
93. I. F. Mirabel: Science **312**, 1759 (2006)
94. I. F. Mirabel, V. Dhawan, R. P. Mignani et al.: Nature **413**, 139 (2001)
95. I. F. Mirabel, L. F. Rodríguez: ARA&A **37**, 409 (1999)
96. I. F. Mirabel, L. F. Rodríguez: Nature **392**, 673 (1998)
97. I. F. Mirabel, V. Dhawan, S. Chaty et al.: A&A **330**, L9 (1998)
98. I. F. Mirabel, L. F. Rodríguez: Nature **371**, 46 (1994)
99. I. F. Mirabel, L. F. Rodríguez, L. F., B. Cordier et al.: Nature **358**, 215 (1992)
100. M. Muno, J. Mauerhan: ApJ **648**, L135 (2006)
101. R. Narayan, M. R. Garcia, J. E. McClintock: ApJ **478**, L79 (1997)
102. R. Narayan, I. Yi: ApJ **444**, 231 (1995)
103. R. Narayan, I. Yi: ApJ **428**, L13 (1994)
104. J. Nichols et al.: ApJ **660**, 651 (2007)
105. J. Poutanen, P. Coppi: Physica Scripta **77**, 57 (1998)
106. J. Rodriguez et al.: ApJ **655**, L97 (2007)
107. M. P. Rupen, A. Mioduszewski, J. L. Sokoloski: ApJ, submitted (2007) [arXiv0711.1142]
108. D. M. Russell, R. P. Fender, E. Gallo et al.: MNRAS **376**, 1341
109. D. M. Russell, R. P. Fender, R. I. Hynes et al.: MNRAS **371**, 1334 (2006)
110. E. S. Rykoff, J. M. Miller, D. Steeghs et al.: ApJ **666**, 1129 (2007)
111. E. R. Seaquist: Radio emission from novae. In: *Classical Novae*, ed by M. F. Bode, A. Evans (Chichester: Wiley) 143 (1989)
112. F. Seward, J. Grindlay, E. Seaquist et al.: Nature **287**, 806 (1980)
113. J. L. Sokoloski, S. J. Kenyon, C. Brocksopp et al.: Jets from Accreting White Dwarfs. In *Revista Mexicana de Astronomia y Astrofisica Conference Series*, vol 20, ed by G. Tovmassian, E. Sion, pp 35-36 (2004)
114. A. M. Stirling, R. E. Spencer, C. J. de la Force et al.: MNRAS **327**, 1273 (2001)
115. L. Titarchuk, T. Zannias: ApJ **493**, 863 (1998)
116. J. A. Tomsick, E. Kalemci, P. Kaaret et al.: ApJ, in press (2008) [arXiv:0802.3357]
117. J. A. Tomsick, S. Corbel, R. P. Fender et al.: ApJ **582**, 933 (2003)
118. J. A. Tomsick, S. Corbel, R. P. Fender et al.: ApJ **597**, L133 (2003)
119. V. Tudose, R. P. Fender, C. R. Kaiser et al.: MNRAS **372**, 417 (2006)
120. M. Watson, G. Stewart, A. King et al.: MNRAS **222**, 261 (1986)
121. F. Yuan, Z. Q. Shen, L. Huang: ApJ **642**, L45 (2006)
122. F. Yuan, W. Cui W., R. Narayan: ApJ **620**, 905 (2005)